OVERVIEW OF AN OPTIMIZED THRUST BALANCE USED FOR ACCURATE MEASUREMENTS IN ELECTRICAL THRUSTER QUALIFICATION ENDURANCE TESTING

Pierre Moutet [(1)], Emmanuel Pouleau [(2)]

[(1)] Physics PhD, DACTEM, 2 Ter rue Marcel Doret, 31700 Blagnac, France
Email: pierre.moutet@dactem.com
[(2)] CEO, DACTEM, 1545 Chemin Sous St Etienne, 30100 Alès, France
Email: emmanuel.pouleau@dactem.com

KEYWORDS: null deflection hanging pendulum thrust stand design qualification endurance testing

ABSTRACT:

This paper presents a null deflection hanging pendulum thrust balance. Based on a previous existing thrust stand, its design has been modified to allow for accurate measurements of thrust ranging from 10 mN to 100 mN. The sensitivity of the thrust stand is less than 70 µN with a resolution better than 350 µN. Intended for qualification endurance testing, the thrust stand can perform continuously for 24 hours, without degrading its performances. Several limitations of the previous design had to be overcome in order to guarantee new performances. Mechanical, thermal, electromagnetics and dynamical studies have been performed by DACTEM. These studies and the resulting design optimization are presented in this paper.

1. INTRODUCTION

Electric propulsion has been under development for more than half a century [1]. Despite providing lower thrust than chemical propulsion systems, electrical propulsion has a vastly superior efficiency, and operates at a higher specific impulse [2]. This render this technology especially interesting for manoeuvres of spacecrafts during orbits, such as attitude control or collision avoidances, or during deep space mission to achieve high velocities. However, their low thrust requires specific equipment during the testing and qualification phases, which has led to a large variety of tests stands being developed over the last 50 years. Most of these stands are based on a pendulum design, allowing to discriminate the weight of the thruster from the low thrust produced. Three types of pendulums exists : inverted [3] [4], hanging [5] and torsional [6] [7]. Each of these configuration has its advantages and disadvantages [8].

This paper presents the detailed design of a hanging pendulum null deflection based test stand, dedicated to a thrust measurement range of 10 mN to 100 mN, and compatible with qualification endurance testing that can last up to 24 hours.

2. EXPERIMENTAL SETUP AND DESIGN CONSTRAINT

The thrust stand is based on a previous existing design, adapted to conform with new specifications from the industry. The target range of thrust measurement has been changed to 10 mN to 100 mN. The resolution of the thrust measurement is expected to be better than 350 µN and its sensitivity less than 70 µN, with a response time under 10 s. During endurance testing, the thermal drift of the test stand has to be under few mN after 24 hours.

Fig. 1 presents CAD views of the test stand. It is composed of a metallic framework (grey) supporting the moving part of the pendulum (dark blue) through flexure joints (yellow). During operations, the thrust generates a displacement of the moving part, away from its original equilibrium position. This movement is quantified by a capacitive displacement sensor, a capaNCDT™ (light blue). Through a feedback loop, the displacement signal is used to power a voltage-driven voice-coil (VC) actuator (pink). It produces a counter thrust, tending to restore the original equilibrium position. Once achieved, the electrical current intensity i used to power the VC is measured. Knowledge of the VC force constant k_e allows to convert i to the thrust produced, by following Eq. 1.

$$Thrust = k_e \times i \qquad \text{Eq. 1}$$

As for all hanging pendulum, the displacement of the moving part of the thrust stand is not straight but slightly curved. Therefore, the effect of gravity must be taken into account in the design. Most specifically, the center of mass of the moving part has to be vertically aligned with the center of rotation in order to minimize the displacement at equilibrium and prevent torque build-up in the flexure joints.

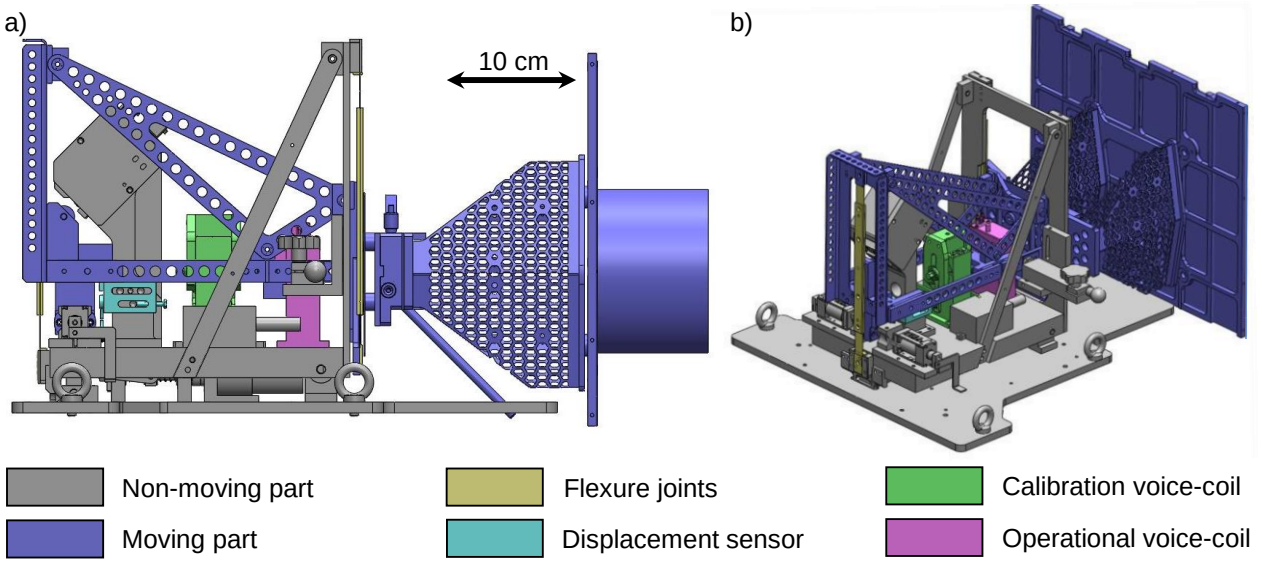

Figure 1 : CAD views of the thrust stand.

Thrusters testing are operated under vacuum. Heat produced by the thruster and the VC will propagate by conduction and radiation, to the thrust stand and its environment. If not properly managed, it can be detrimental for the performances of the thrust stand through a large variety of phenomena. This is especially true for endurance testing which last for many hours. For instance, thermal expansion of the mechanical parts can generate a significant drift in the thrust measurement. The sensitivity of the displacement sensor is also affected by the temperature. And the change of conductivity of the copper wire of the VC would modify its force constant, introducing an error in Eq. 1 that could be significant.

As stated, the displacement of the moving part is regulated by a feedback loop, integrating a PI regulator. Consequently, the transient response of the thrust stand is strongly depending on the parameters of the PI regulator. As such, the stability of the thrust stand depends on its transfer function. If not carefully monitored, change in the design could lead to an instable system, regardless of the parameters of the PI regulator.

In order to address all potential issues, thorough studies have been achieved during the design phase. Results are presented in the following sections.

3. MODELING AND ANALYSIS OF THRUST STAND

CAD of the thrust stand was achieved using SOLIDWORKS, mechanical, thermal and electromagnetic simulations were performed using ALTAIR™ finite element method (FEM) software, respectively SIMLAB™, ACUSOLVE™, and FLUX™. Lastly, dynamical studies were carried out using SCILAB with Xcos module.

3.1. Mechanical engineering

As the weight of the target thrusters are dissimilar between the previous and the current design, multiples mechanical adjustments are in order. Especially, the center of mass of the moving

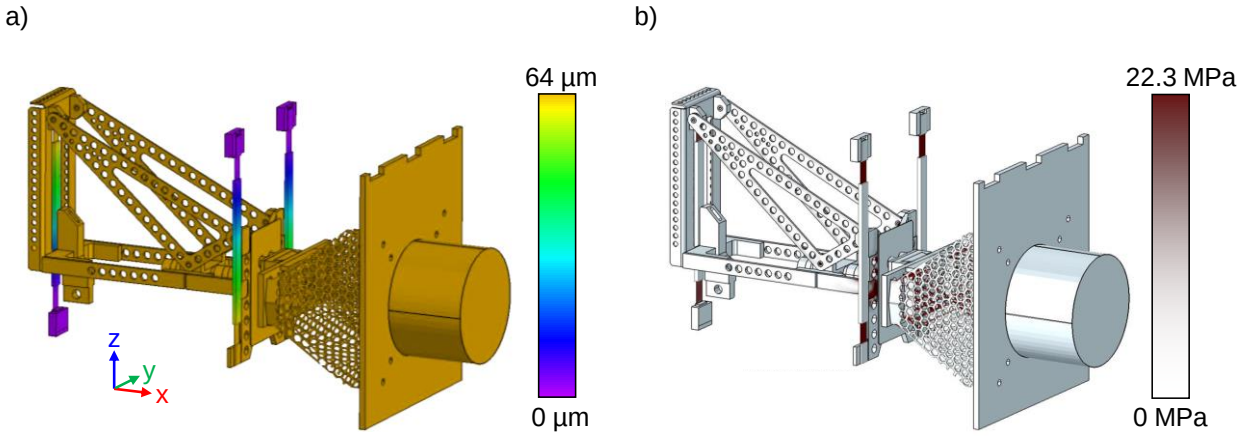

Figure 2 : FEM simulation of a) the displacement and b) mechanical stress of the moving part at 65 mN thrust.

part has to be vertically aligned with the center of rotation. To equilibrate the moving part, which include the tested thruster, the mobile mass is reduced from 39 kg to 12 kg. It is achieved by adding through-holes in various location of the moving parts of the thrust stand, and changing materials to reduce their density. This last process is balanced between weight gain, frame stiffness, and thermal management constraints (see 3.3).

During modifications of the design, studies were performed to ensure that the quantity of displacement of the moving part generated by the thrust was sufficient enough with regards to the selected displacement sensor. Fig.2a presents the displacement of the moving part of the thrust stand for a 65 mN thrust. Purple indicate a lack of displacement, while dark yellow correspond to a 64 µm displacement along the negative direction of the X axis. As intended, this value is compatible with the 1 mm range of the displacement sensor. Moreover, the corresponding displacement for the target thrust sensitivity of 70 µN can be estimated by linear regression to 68 nm. This value is highly superior to the 0.75 nm sensitivity of the displacement sensor.

Fig.2b presents, for a 65 mN thrust, the mechanical stress generated. It reaches a value of 14.7 MPa inside all flexure joints. This value ensures a large safety margin from the 206.8 MPa yield stress of the stainless steel 304L. A maximum value is recorded inside the fixture joints of the thruster mount, where constraints are concentrated up to 25.4 MPa, resulting again in a significant safety margin.

3.2. Electromagnetic engineering

The previous thrust stand integrated a VC designed with an AlNiCo magnet and a copper coil. It presented three major issues : (1) the AlNiCo self-demagnetization was not anticipated, (2) the coil had a small section assembled with a 0.2 diameter wire and (3) it was a moving coil design. (1) led to a significant 65% reduction of the VC force constant, from 2.64 N/A to 0.925 N/A. To compensate, the current required to counter the thrust had to be increased by the same amount. (1) combined with (2) led to a strong joule heating of the copper coil, resulting in a noticeable thrust drift during all of performed measurements. Lastly, (3) complexified the heat dissipation of the coil, whilst moving wires generated parasitic stiffness, detrimental to the performances of the thrust stand.

To prevent such issues, a new VC is designed using guideline from the literature [9], tailored toward the anticipated performances of the thrusters. It is based on a moving magnet design, with the magnetic material changed to SmCo, chosen for its insignificant self-demagnetization. Two magnets are integrated, mounted with opposite magnetic orientations to coerce a transverse orientation of the magnetic field B throughout the coil, enabling the Lorentz force to be maximised. Comparison of the magnetic fields and geometries of the previous and current VCs are presented in Fig. 3.

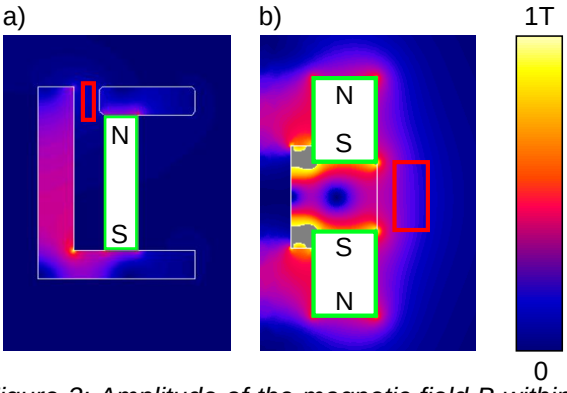

Figure 3: Amplitude of the magnetic field B within : a) VC of the previous thrust stand (b) VC of the current thrust stand.

The red outlined rectangles of Fig. 3 represents sections of the copper coil, while the green outlined rectangles represents magnets of the VCs. Magnetic orientations are indicated with the N and S letters. The transversal component of the magnetic field in coil of the previous and the current design reaches respectively an amplitude of 113 mT and 285 mT, an improvement of 250%. Combining the magnetic field with an increase of the surface of the coil from of 7.35 mm² to 32 mm² and a decrease of the wire diameter to 0.63 mm result in a final force constant of the new VC of 1.47 N/A. Thus, despite a 60% improvement of the force constant, the current design offer a reduction of the maximum operational Joule heating from 880 mW to 4 mW. This result enabled the VC produced calories to be ignored during thermal studies.

3.3. Thermal engineering

Thermal engineering aims at managing calories during operational activities, in order to limit its spread inside the moving part of the thrust stand. As seen in 3.2, the Joule heating of the VCs is drastically reduced. Thermal studies show that only the calories generated by the thruster remains significant and need to be managed. To this end, a two steps approach is used : (1) limiting the propagation of calories produced by the thruster into the moving part, (2) increasing the dissipation of calories by radiation.

To address (1), the thruster mount is redesigned. Modifications are presented in Fig. 4. Fig. 4 a. and b respectively shows the previous and current thruster mount. Through-holes are added to generate a decrease of the conduction section and an elongation of the conduction

pathway. These changes result in a 38% decrease of the thermal conductivity. Moreover, theses holes reduce the mass of the moving part, addressing the issues discussed in 3.1. Both previous and current thruster mount are in stainless steel 304L, as changing the material was not necessary.

Parts made of zirconium dioxide are added in interface where mechanical constraints need to be managed while providing thermal isolation. This ceramic has a thermal conductivity of 2.2 $W.m^{-1}.K^{-1}$ and a yield stress of 250 MPa, which are compatible with our application. Moreover, sheets of cork-based insulators are added when no mechanical loads occurs. In the past, such insulators have successfully been used in several space flight vehicles [10]. The selected material for this project has an excellent thermal conductivity of 0.045 $W.m^{-1}.K^{-1}$.

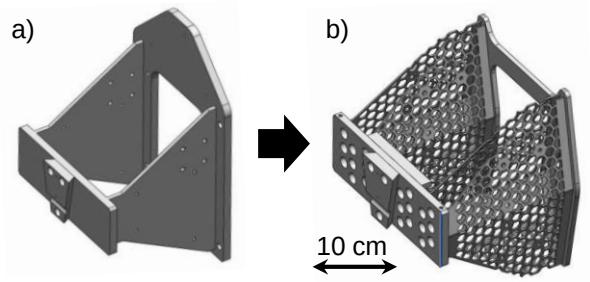

Figure 4 : CAD views of the thruster mount of (a) the previous thrust stand and (b) the current thrust stand.

The emissivity coefficient of the stainless steel surface is improved by corundum sandblasting. With regard to the current literature [11], the treatment is expected to double the emissivity of the material. This improvement combined with the increased of material surface granted by the holes, allow to maximise the dissipation of calories through radiations.

The result of the thermal design optimization is presented in Fig. 5. Fig. 5.a displays, for a 20 °C environmental temperature, the thermalisation of the thrust stand with a temperature of 50°C of the thruster. The FEM simulation of the thermalisation after 24 hours clearly demonstrate that the redesigned thruster mount is drastically restricting the propagation of the calories inside the moving part, limiting the increase of temperature to less than 1°C to the rest of the thrust stand.

At the displacement sensor location, the thermal dilatation of the thrust stand generates an error of -1.41 µm, corresponding to a thermal drift of 1.44 µN. This excellent result is few orders of magnitude better than the target specification, ensuring good stability during qualification endurance testing.

Fig. 5.b presents the variation of temperature at the displacement sensor location. It can be noted that 98% of the thermalisation is achieved after 13 hours. At the displacement sensor location, an increase of 0.97°C is registered, resulting in a decrease of the sensor sensitivity of 23 nm.

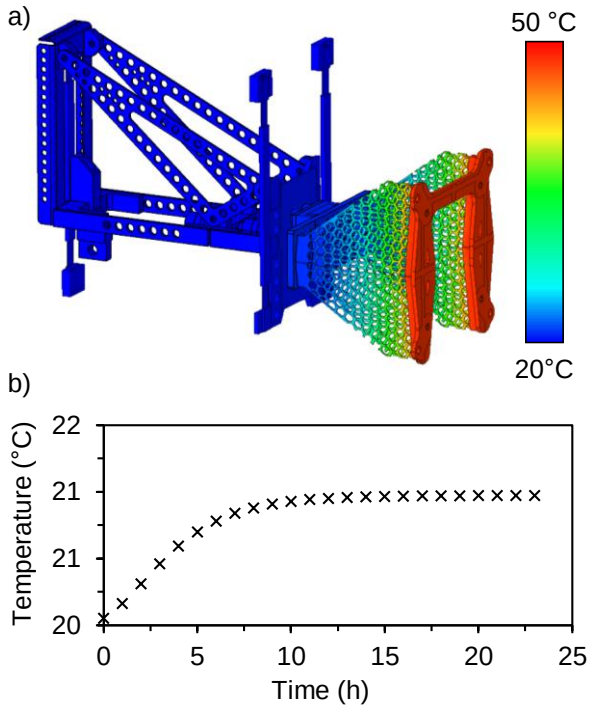

Figure 5 : a) FEM simulation of the thermalisation after 24h at 65 mN thrust and (b) variation of temperature at the displacement sensor location.

3.4. Dynamical behaviour

The transient response of the system and its stability in closed-loop is studied.

Table 1 : Value used for the simulation

Constant	Description	Value	Units
m	Mass of the moving part	12	kg
g	Gravitational constant	9.81	$m^3.s^{-1}.kg^{-2}$
l	Length of resulting global flexure joint	0.18	m
k	Global mechanical stiffness	133	$N.m^{-1}$
L	Inductance of operational VC	0.28	mH
R	Resistance of operational VC	0.43	Ω
ke	Force constant of operational VC	2	$N.A^{-1}$
L_{VC}	Inductance of calibration VC	0.28	mH
R_{VC}	Resistance of calibration VC	0.43	Ω
ke_{VC}	Force constant of calibration VC	2	$N.A^{-1}$
k_p	Proportional gain of the PI regulator	2000	-
K_i	Integral gain of the PI regulator	1000	-

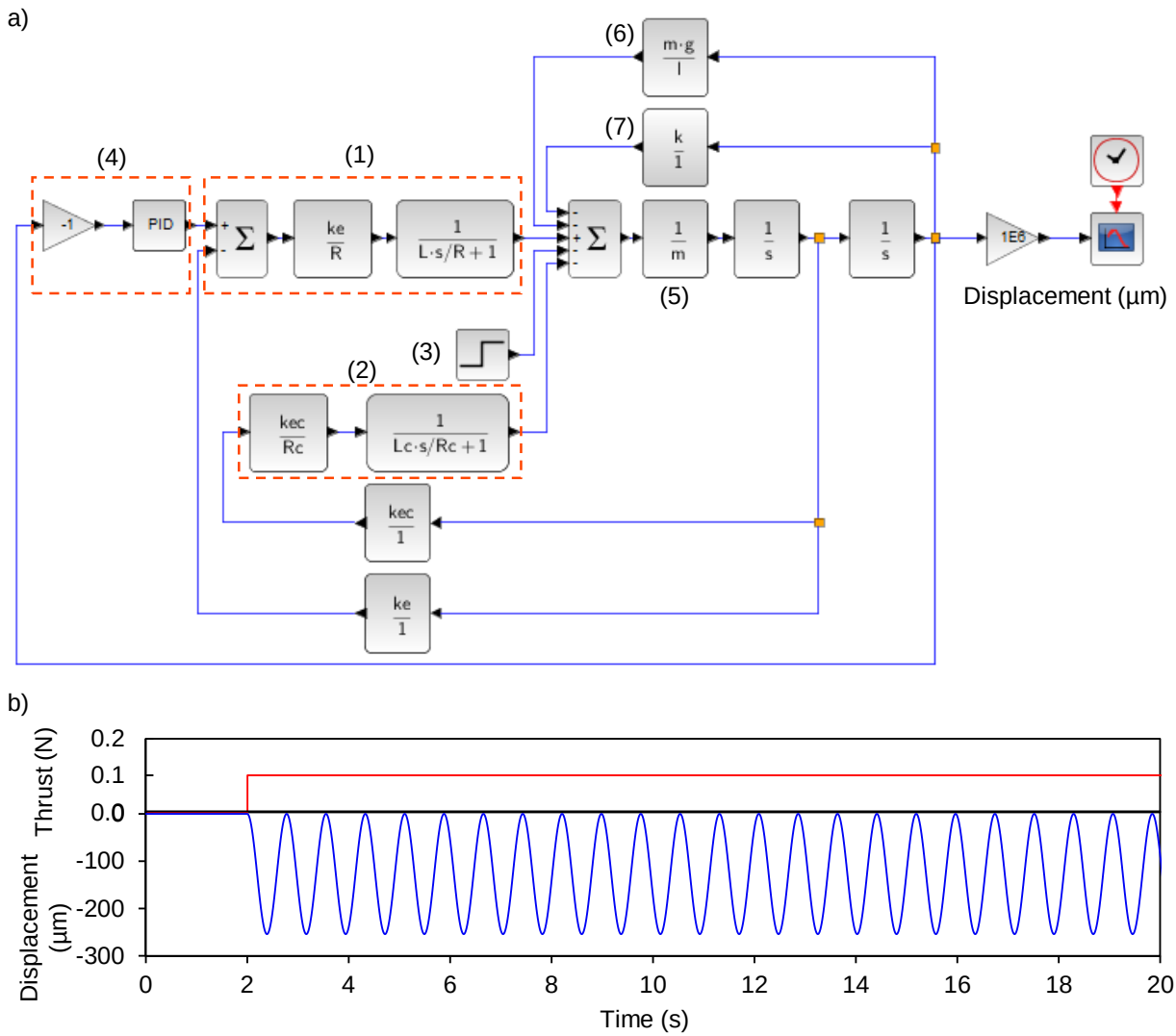

Figure 6: a) SCILAB block diagram of the thrust stand in closed-loop and b) displacement at the sensor location (bottom) for a 100 mN step of thrust (top).

Fig 6 presents the simulation of the step response of the thrust stand. Parameters values are summarized in Tab.1.

Fig 6.a presents the SCILAB bloc diagram of the thrust stand. It includes: (1) the force produced by the powered and voltage driven operational VC, (2) damping generated by the unpowered calibration VC, (3) thrust of the thruster, (4) feedback loop, (5) effect of the mass of the moving part of the thrust stand, (6) gravity and (7) global equivalent stiffness of the mechanism.

The mechanism of the thrust stand is simplified to a 2D system composed of a mass *m* hanged to a rigid pivot of length *l* and stiffness *k*. Transversal forces applied to the suspended mass by (1) and (3) tend to move it away from its equilibrium position, while (2) (6) and (7) tends to bring it back.

Fig 6.b present the result of the simulation. The red curve shows a 100 mN thrust starting at t=2 s. The blue curve is the corresponding displacement measured by the sensor. As expected, as soon as the 100 mN thrust is applied, a negative displacement occurs, reaching a value of -19.1 µm at t=2.11 s. Damped oscillations of the moving part are then produced, with a frequency of 4.7 Hz. After t=9.05s, only 10% of the amplitude of the first oscillation remains, corresponding to a settling time of 7.05 s.

It is important to note that the step response of the thrust stand can be modified by changing the K_p and K_i values of the feedback regulator. Fine tuning of theses parameters will take place during the integration phase.

This simulation could be further improved if needed. For instance, the displacement sensor and all analogic electronics could be implemented. Likewise, studies are under progress to elaborate a simulation of the system combining all FEM results previously presented that would be relevant for predicting the dynamical behaviour of the system, such as the mechanical and electromagnetic simulations.

Nonetheless, preliminary results displayed in Fig 6 are sufficient enough to validate the design of the system and its ability to perform after proper tuning of the PI regulator.

4. CONCLUSION

An existing hanging pendulum null deflection thrust stand has been redesigned to improve and adjusts its performances. The new range of thrust measurement span from 10 mN to 100 mN, with a resolution better than 350 µN and the sensitivity less than 70 µN. To ensure theses performances, various limitations of the previous design had to be overcome.

First, the weight of the moving part was reduced from 39 kg to 12 kg. Flexure pivots were redesigned, and mechanical stress within sensitives parts studied. Results shows that constraints are concentrated up to 25.4 MPa, ensuing in a significant safety margin from the 206.8 Mpa yield stress.

The voice-coil actuator of the thrust stand was entirely modified, switching to a moving magnet design. The material was changed to SmCo in order to prevent self-demagnetization. Results show a 60% improvement of the force constant, with a reduction of the joule heating from 880 mW to 4 mW at maximum thrust.

Thermal management of the calories produced by the thrust was performed, to ensure performances of the thrust stand during endurance testing. By redesigning the thruster mount, the conduction of the calories to the moving part of the thrust stand was slowed. Ceramics were integrated to similar intent. A 80% decrease of the propagation rate of the calories was achieved. Furthermore, by increasing the surface of the thruster mount and doubling its surface emissivity with corundum sandblasting, the dissipation of calories by radiation was drastically improved. For a 65 mN thrust, results show a thermalisation of the thrust stand after 13h and a thermal drift of less than 2 µN.

At last, dynamical behaviour in closed loop of the thrust stand was investigated. Good stability was demonstrated and a response time under 8s.

Integration of the thrust stand is under progress at DACTEM headquarters. Acceptance testing are planned for first semester of 2021.

5. ACKNOWLEDGEMENT

The thrust stand development activities were achieved with the trust and support of SAFRAN Aircraft Engines as well as the Région Occitanie and internal funding.

[1] M. Martinez-Sanchez and J. E. Pollard, ‘Spacecraft Electric Propulsion-An Overview’, *Journal of Propulsion and Power*, vol. 14, no. 5, pp. 688–699, Sep. 1998, doi: 10.2514/2.5331.

[2] P. Erichsen, ‘Performance Evaluation of Spacecraft Propulsion Systems in Relation to Mission Impulse Requirements’, vol. 398, p. 189, Aug. 1997.

[3] A. Neumann, J. Sinske, and H.-P. Harmann, ‘The 250mN Thrust Balance for the DLR Goettingen EP Test Facility’, Jan. 2013, pp. 1–10.

[4] U. Kokal, ‘Development of a Mili-Newton Level Thrust Stand for Thrust Measurements of Electric Propulsion Systems and UK90 Hall Effect Thruster’, 2018.

[5] K. A. Polzin, T. E. Markusic, B. J. Stanojev, A. DeHoyos, and B. Spaun, ‘Thrust stand for electric propulsion performance evaluation’, *Review of Scientific Instruments*, vol. 77, no. 10, p. 105108, Oct. 2006, doi: 10.1063/1.2357315.

[6] Y.-X. Yang, L.-C. Tu, S.-Q. Yang, and J. Luo, ‘A torsion balance for impulse and thrust measurements of micro-Newton thrusters’, *Review of Scientific Instruments*, vol. 83, no. 1, p. 015105, Jan. 2012, doi: 10.1063/1.3675576.

[7] T. W. Haag, ‘Thrust stand for pulsed plasma thrusters’, *Review of Scientific Instruments*, vol. 68, no. 5, pp. 2060–2067, May 1997, doi: 10.1063/1.1148097.

[8] J. E. Polk *et al.*, ‘Recommended Practice for Thrust Measurement in Electric Propulsion Testing’, *Journal of Propulsion and Power*, vol. 33, no. 3, pp. 539–555, 2017, doi: 10.2514/1.B35564.

[9] ‘Contributed Review: Application of voice coil motors in high-precision positioning stages with large travel ranges: Review of Scientific Instruments: Vol 86, No 10’. https://aip.scitation.org/doi/10.1063/1.4932580 (accessed Nov. 22, 2020).

[10] O. Drescher, M. Hörschgen-Eggers, G. Pinaud, and M. Podeur, ‘Cork based thermal protection system for sounding rocket applications - Development and flight testing’, presented at the 23rd ESA PAC Symposium, Jun. 2017.

[11] P. Demont, H. T. Nguyen, and J. F. Sacadura, ‘INFLUENCE DE L’OXYDATION ET DE LA RUGOSITÉ SUR LES CARACTÉRISTIQUES RADIATIVES DES ACIERS INOXYDABLES’, *J. Phys. Colloques*, vol. 42, no. C1, pp. C1-161-C1-171, Jan. 1981, doi: 10.1051/jphyscol:1981111.